

Available online at www.sciencedirect.com**ScienceDirect**

Energy Procedia 79 (2015) 272 – 277

Energy

Procedia

2015 International Conference on Alternative Energy in Developing Countries and Emerging Economies

Reduction of Electrode Polarization in Anode-Supported Solid Oxide Fuel Cell

Malinee Meepho^a, Darunee Wattanasiriwech^a, Pavadee Aungkavattana^b,
Suthee Wattanasiriwech^{a*}

^aMae Fah Luang University, Chiangrai, 57100, Thailand

^bNational Metal and Materials Technology Centre, 12120, Thailand

Abstract

In this work, an attempt to reduce electrode polarization of an anode-supported solid oxide fuel cell with two approaches and the improvement of the cell electrochemical performance is reported. In fabrication of a conventional single solid oxide fuel cell, yttria stabilized zirconia (8YSZ), NiO-8YSZ, and lanthanum strontium cobalt fluorite (LSCF) were used as electrolyte, anode and cathode materials. On the pre-fired porous anode support, the electrolyte was deposited by electrophoresis deposition while the cathode layer was deposited using a screen-printing method. The first approach was performed by a deposition of samaria doped ceria (SDC) interlayer to prevent formation of an insulating phase between 8YSZ/LSCF interface, while the second approach involved adjustment of the anode microporous structure. The electrochemical performance of the fabricated cells was characterized using an impedance spectroscopy technique. The results showed that insertion of the interlayer between the LSCF cathode and YSZ electrolyte could prevent insulating phase formation, giving rise to a significantly decrease in polarization resistance and a much improved power density over the reference cell. In addition, the anode polarization was further reduced with pore enlargement in the anode substrate together with the fine microstructure of anode functional layer.

© 2015 The Authors. Published by Elsevier Ltd. This is an open access article under the CC BY-NC-ND license (<http://creativecommons.org/licenses/by-nc-nd/4.0/>).

Peer-review under responsibility of the Organizing Committee of 2015 AEDCEE

Keywords: Solid Oxide Fuel Cells; Electrophoresis Deposition; Impedance Spectroscopy; Interlayer

1. Introduction

Solid oxide fuel cells (SOFCs) have been proposed to be one of the key energy resources for the future due to their promising efficiency, environmental friendliness, fuel flexibility and low chemical, particulate and noise emission as well as size compaction [1-2]. Operation of cells was based on

*Corresponding author. Tel.: +66-53-91-6263; fax: +66-53-91-6776.
E-mail address: suthee@mfu.ac.th

electrochemical reaction between a fuel and an oxidizing agent, principally oxygen resulting in water and electrical power. Conventionally SOFCs were operated at around 800-1000°C to obtain satisfactory ionic conductivity of the electrolyte layer. This high temperature operation could in turn cause undesirable effects such as high corrosion rate of the cell components and cost ineffectiveness. Lowering the operation temperatures to the intermediate range (600-800°C) by reducing the electrolyte thickness was one way forward to solve this problem.

SOFCs with a porous anode supported design were extensively studied as they showed lower ohmic resistance [3]. In this design configuration, a thin electrolyte film was deposited on the pre-fired porous anode, typically made of Ni/8YSZ composite and co-fired at the electrolyte sintering temperature. The challenge was to maintain porous anode feature while densifying only the electrolyte layer. This cell design was prone to electrolyte cracking during manufacturing due to high thermal expansion coefficient of the NiO compared to that of zirconia electrolyte [1]. Fabrication of this cells based on this design must therefore be done with great care. As the ohmic losses could be greatly reduced in anode supported design, the overall polarization was governed by electrode polarization, depending on the conductivities of anode, cathode and electrolyte/electrode interface. Interaction at 8YSZ-LSCF interface resulting dense insulating phase was reported to inhibit ion transportation across interface. Insertion of a ceria based electrolyte interlayer could prevent an undesirable interfacial reaction [4].

The anode supported design was based on thick anode layer which, however, could contribute greatly to electrode polarization. It was reported that the ideal microstructure of porous anode support was a continuously transitional structure with a thick porous layer of big pores and a thin porous layer of small pores [5]. From our previous results [6], the addition of anode functional layer which exhibited finer microstructure could increase activity at the electrolyte/anode interface. However, a significant electrode polarization resistance of the other components in the cells was still observed [6] due to the interaction between LSCF cathode and 8YSZ electrolyte, giving rise to formation of $\text{La}_2\text{Zr}_2\text{O}_7$ and SrZrO_3 phases at the cathode-electrolyte interface [7].

Electrophoresis deposition (EPD) is a technique widely used in fabrication of ceramic thin films [8]. It provides many advantages such as short formation time, little restriction in the shape of deposition substrate, suitability for mass production, and ease of thickness control [9]. In this study, the electrolyte layer with the thickness less than 10 μm was fabricated by EPD. Attempts to reduce electrode polarization of the cells by (i) insertion of the samaria doped ceria (SDC) interlayer and (ii) adjusting the anode microstructure were addressed.

2. Methodology

Three different cell designs were studied and were coded as follows;

- Cell-A: anode support, anode functional layer | | electrolyte | | LSCF cathode
- Cell-B: anode support, anode functional layer | | electrolyte | | SDC interlayer, LSCF cathode
- Cell-C: anode support, anode functional layer | | electrolyte | | SDC interlayer, LSCF cathode

The anode support was prepared by mixing NiO (Fuel Cell Materials, America) and 8YSZ powders (TOSOH, Japan) at a weight ratio of 50:50. Corn starch (15 wt% of the total solid) was used as the pore former. The anode mixture was milled for 24 h (Cell-A and Cell-B) and 1 h (Cell-C) to obtain two different microstructures. The anode support was subsequently pre-sintered at 900°C for 4 h. The anode functional layer was prepared by dispersion of mixed NiO and 8YSZ powders at the weight ratio of 60:40 in absolute ethanol. The suspension was prepared with powder loading of 10 g/L and ultrasonicated for 30 min before the EPD process at 30 V for 1 min, followed by sintering at 800°C for 2h. The electrolyte layer was then electrodeposited on the top of the functional layer at 30 V for 2 min. These layers were co-sintered at 1400°C for 2 h with a heating rate of 1°C/min. The SDC paste was prepared by mixing the

SDC powder with terpenol at the wt. ratio of 65:35. The SDC paste was then screen-printed onto the surface of sintered electrolyte, followed by drying at 60°C and subsequently sintering at 1200 °C for 2 h to obtain an optimal contact with the electrolyte. The thickness of the sintered SDC interlayer was approximately 50 µm. To prepare LSCF cathode, $\text{La}_{0.6}\text{Sr}_{0.4}\text{Fe}_{0.8}\text{Co}_{0.2}\text{O}_3$ (LSCF, American Elements) powder was mixed with terpenol at the weight ratio of 60:40 by hand grinding to form LSCF cathode paste. LSCF paste was then screen-printed onto the electrolyte side, followed by drying at 60 °C and subsequently sintering at 1100°C for 2 h in order to obtain sufficient contact with the electrolyte. The thickness of the sintered LSCF cathode was about 40 µm. Pt mesh was then glued to the cathode side while Pt wire was used as the current collector. The electrochemical performance was measured with hydrogen as the fuel and oxygen as the oxidant at 800 °C. To distinguish different loss mechanisms, the single cell was characterized using impedance gain/phase analyzer (Solartron 1260) under an open circuit condition. Microstructure and morphology of the fabricated cells both before and after the performance tests were examined by a scanning electron microscopy attached with an EDS.

3. Results and discussion

3.1. Effects of SDC interlayer addition

Cross-sectional microstructure of Cell-A and Cell-B are displayed in Fig 1. For Cell-A, the dense insulating phase was clearly observed at 8YSZ/LSCF interface. Addition of SDC interlayer (Cell-B) could inhibit the formation of this interface phase. The distributions of Ni, Zr, and Ce elements determined using an EDX mapping over the Ni-8YSZ/8YSZ/SDC interfaces confirmed the absence of atomic interdiffusion between the components in Cell-B. However, it can be seen that the interlayer was not fully densified due to the use of relatively low sintering temperature (1200 °C) to avoid formation of resistive $\text{CeO}_2\text{-ZrO}_2$ phase [10].

Figure 2 shows the electrochemical performance of Cell-A and Cell-B measured at 800 °C under open circuit potential conditions using hydrogen as fuel and air as oxidant. The result indicated that the presence of SDC interlayer (in Cell-B) could enhance the electrochemical performance, as compared to that of Cell-A. The maximum power densities obtained from Cell-A and Cell-B were 2.1 and 7.4 mW/cm², respectively.

Electrochemical impedance spectra of Cell-A and -B measured at 800°C are shown in Fig 3. It Cell-B exhibits a much lower electrode polarization resistance than Cell-A, correlating with the improvement of electrochemical performance as shown in Fig 2. In contrast, it should be noted that the ohmic resistance of Cell-B was much greater than that of Cell-A. The fully densified 8YSZ electrolyte layer had the ohmic resistance of only 3 ohms [6], so such a high ohmic resistance was thus according to the porous SDC interlayer in Cell-B.

Therefore it could be concluded that the SDC interlayer introduced in Cell-B could help reduce the electrode polarization by preventing the formation of dense interfacial layer between the 8YSZ electrolyte and the LSCF cathode. This result also correlated with the improved cell power density obtained from cell-B.

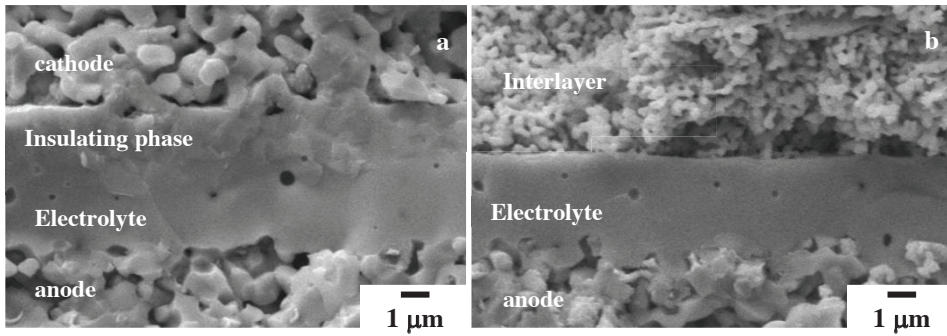


Fig. 1. Cross-sectional SEM images for (a) Cell-A; (b) Cell-B

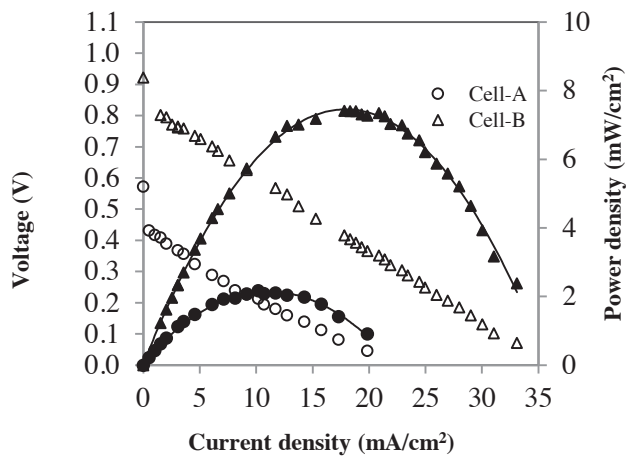


Fig. 2. Electrical performances of Cell -A and Cell-B measured at 800 °C

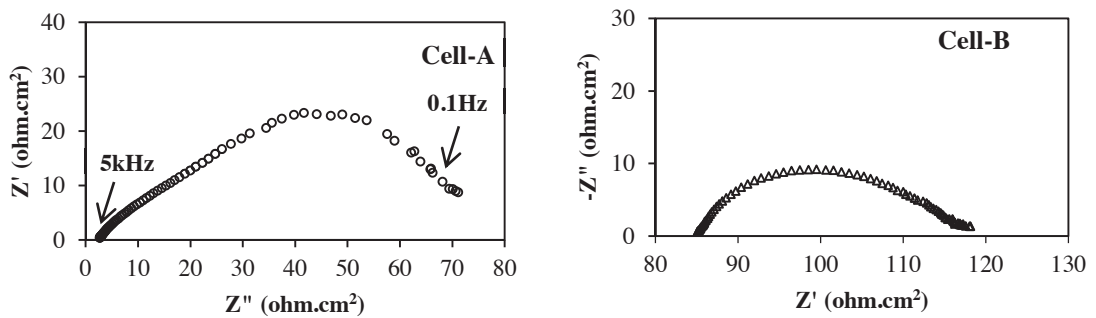


Fig. 3. Electrochemical impedance spectra of Cell-A and Cell-B measured at 800°C.

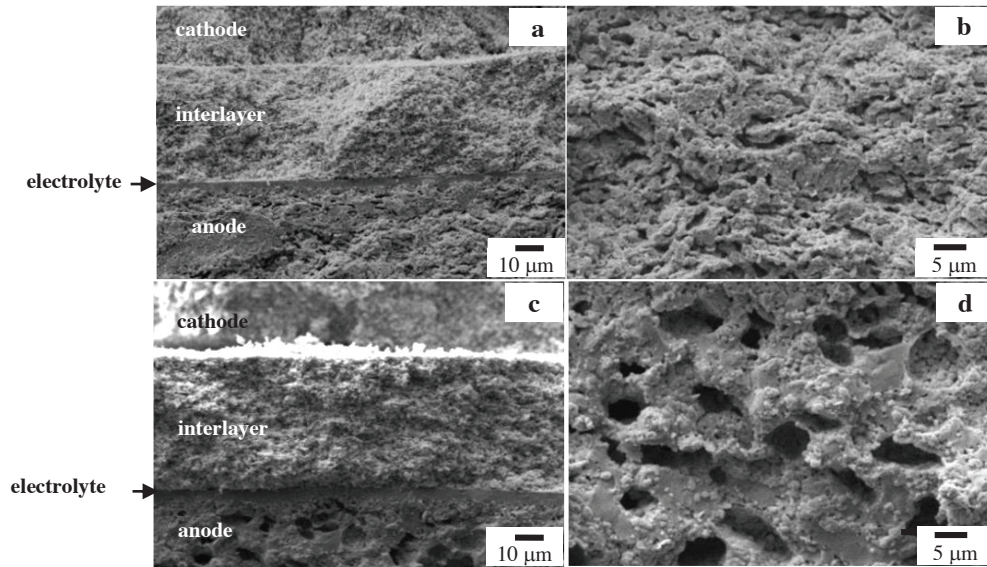


Fig. 4. Cross-sectional SEM images of (a) cell-B; (b) Ni-8YSZ anode milled 24 h; (c) cell-C, and (d) Ni-8YSZ anode milled for 1 h

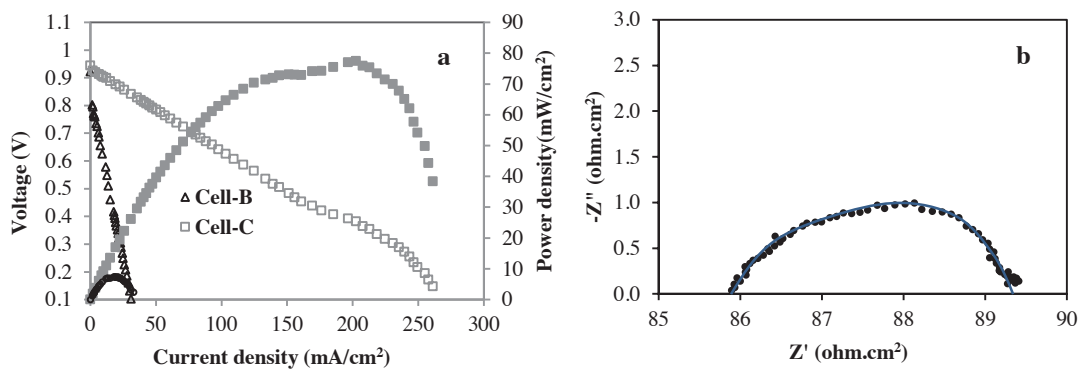


Fig. 5. (a) Electrical performance of Cell-B and Cell-C in comparison; (b) Electrochemical impedance spectra of cell-C. The measurement was performed at 800°C.

3.2 Effect of anode microstructure

Comparative microstructures of Cell-B and Cell-C are displayed in Fig 4. The pore morphology of the anode support in Cell-C was, in general, spherical, suggesting that 1-h milling could only slightly cause deformation of the corn starch. The pore size distribution was relatively uniform with a diameter around 10 μm . Pore morphology of the anode support in Cell B was flattened and much smaller in size.

Electrochemical performance of cell-B and cell-C measured at 800 °C are shown in Fig 5. It can be seen that an enhancement in cell performance, with the maximum power density of 77 mW/cm^2 , was achieved for Cell-C. The better cell performance could be explained by the presence of large anode pore

size which was beneficial to gas phase transport. Although it was reported that when pores were relatively big, Ni particles were separated from each other, and led to the increases of ohmic resistances and the decreases of electrochemical activity [11]. However, the electrochemical activity could be increased by addition of anode functional layer with finer microstructure. In addition, it was reported that the electrochemical reaction only occurred within about 10 μm of the anode/electrolyte interface. Thus, the thickness of anode support served only as a mechanical support and a current collection.

The increase in performance was also observed in the impedance spectrum of Cell-C in Fig 5(b). The polarization resistance of this cell was only $\sim 3 \text{ ohm.cm}^2$ which was much lower than that of cell-B which was $\sim 32 \text{ ohm.cm}^2$.

4. Conclusion

Attempts to improve electrode polarization were performed using two strategic approaches; addition of an interlayer and adjusting the anode microstructure. Addition of the SDC interlayer between the LSCF cathode and 8YSZ electrolyte could prevent formation of SrZrO_3 insulating phases. The results showed that the polarization resistance was decreased as compared to the cell without the SDC interlayer. However, thick, unsintered SDC interlayer in turned resulted in higher ohmic resistance of the cell. The polarization of anode substrate was further minimized by enlarging pore size of the anode substrate together with inserting of a thin, fine microstructure anode functional layer. An enhancement in cell performance could be achieved.

Acknowledgement

The authors are grateful for financial support from Thailand Graduate Institute of Science and Technology and Mae Fah Luang University, Thailand.

References

- [1] Badwal SPS, Giddey S, Munnings C, Kulkarni A. Review of progress in high temperature solid oxide fuel cells. *J Aust Ceram Soc* 2014; **50**[1]: 23–37.
- [2] Webe A, Ivers-Tiffée E. Materials and concepts for solid oxide fuel cells (SOFCs) in stationary and mobile applications. *J Power Sources* 2004; **127**: 273–83.
- [3] Singhal SC, Kendall K. *High-temperature solid oxide fuel cells: fundamentals, design and applications*: Elsevier; 2003.
- [4] Kim WH, Song HS, Moon J, Lee HW. Intermediate temperature solid oxide fuel cell using $(\text{La,Sr})(\text{Co,Fe})\text{O}_3$ -based cathodes. *Solid State Ionics* 2006; **177**: 3211–3216.
- [5] Jin C, Yang C, Chen F. Effects on microstructure of NiO–YSZ anode support fabricated by phase-inversion method. *J Membrane Sci* 2010; **363**: 250–255.
- [6] Meepho M. *Preparation of 8YSZ electrolyte film on NiO-8YSZ substrate using an electrophoretic deposition process*. PhD Thesis; Mae Fah Luang University, Thailand; 2013.
- [7] Simmer SP, Shelton JP, Anderson MD, Stevenson JW. Interaction between La (Sr) FeO_3 SOFC cathode and YSZ electrolyte. *Solid State Ionics* 2003; **161**: 11–18.
- [8] Besra L. Electrophoretic deposition on non-conducting substrates: the case of YSZ film on NiO–YSZ composite substrates for solid oxide fuel cell application. *J Power Sources* 2007; **173**:130–136.
- [9] Meepho M, Wattanasiriwech S, Aungkavattana P, Wattanasiriwech D. Application of 8YSZ nanopowder synthesized by the modified solvothermal process for anode supported solid oxide fuel cells *J Nanosci and Nanotech* 2015; **15** [1–5]: 2570–2574.
- [10] Lu Z, Zhou XD, Fisher D, Templeton J, Stevenson J, Wu N, Ignatiev A. Enhanced performance of an anode-supported YSZ thin electrolyte fuel cell with a laser-deposited $\text{Sm}_{0.2}\text{Ce}_{0.8}\text{O}_{1.9}$ interlayer. *Electrochem Comm* 2010; **12**: 179–182.
- [11] Talebi T, Haji M, Raissi B. Effect of sintering temperature on the microstructure, roughness and electrochemical impedance of electrophoretically deposited YSZ electrolyte for SOFCs. *Inter J. Hydrogen Energy* 2010; **35**: 9420–9426.